Image Noise and Colorimetric Precision in Multispectral Image Capture

*Peter D. Burns and Roy S. Berns**
Eastman Kodak Company, Rochester, NY
**Munsell Color Science Laboratory,*
Chester F. Carlson Center for Imaging Science
Rochester Institute of Technology
Rochester, NY

Abstract

The performance of a multispectral (more than three color-records) camera is addressed from the standpoint of pixel-to-pixel error introduced by image detection. Matrix equations are given for the propagation of this image noise from camera signal through colorimetric transformations. Results of the analysis are shown to agree with experimental results, allowing the prediction of system colorimetric precision.

Introduction

Much has been reported recently on the uses of multispectral (more than three color-records) image capture for color-imaging applications.[1-3] Experimental cameras have been described,[3-5] as have the results of signal processing to extract useful spectral and colorimetric information. In general, the emphasis in the field has been on the *accuracy* of the acquisition system and corresponding analysis. Practical systems, however, are subject to both random pixel-to-pixel and calibration errors. This image noise, in addition to signal quantization, influences the *precision* of the system.

Camera System

For applications not requiring simultaneous acquisition of all records, such as document or artwork imaging, a multispectral camera can be formed by acquiring several frames using a set of spectral filters. A set of seven commercially available filters, manufactured by Melles Griot, was used with a (monochrome) Kodak Professional DCS 200mi digital camera. The filter set was chosen because of its wide availability, and approximately equal-interval sampling (50 nm) of the visible wavelength range. This spectral sampling does not favor the characteristics of any particular radiation sources, nor class of object spectra, (e.g., manufactured colorants or natural objects). The digital camera analyzed in conjunction with the filter set yields the combined spectral responses given in Fig. 1.

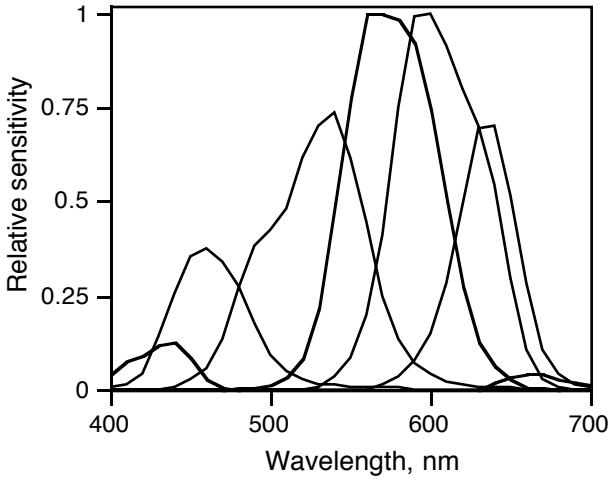

Figure 1: The spectral sensitivity of each of the seven filter/sensor channels.

As previously reported,[5] principal component analysis can be used to reconstruct spectral reflectance curves from camera signals. A least-square matrix, $\mathbf{M}$, was calculated to allow the seven camera signals, $\{s\}$, to be transformed to estimates of the scalar coefficients associated with the eigenvectors, $\{e\}$, to reconstruct the spectra. The spectral reconstruction from n signals using m eigenvectors, expressed in matrix notation, is given by

$$\mathbf{f} = \phi\mathbf{M}\mathbf{s}, \qquad (1)$$

where $\mathbf{f}$ is the reconstructed spectral reflectance vector, $\mathbf{S}^{\mathrm{T}} = [s_1, s_2, \ldots, s_n]$, $\phi^{\mathrm{T}} = [e_1, e_2, \ldots, e_m]$. For specified viewing conditions the CIE tristimulus values, $\mathbf{t}^{\mathrm{T}} = [X, Y, Z]$, for each pixel can be computed using an ASTM weight vector.[6] This is given by $\mathbf{t} = \mathbf{W}\mathbf{f}$, where $\mathbf{W}$ is the weight vector. Combining this operation with that of Eq. (1), the tristimulus vector, $\mathbf{t}$, can be computed from the seven camera signals

$$\mathbf{t} = \mathbf{W}\phi\mathbf{M}\mathbf{s}. \qquad (2)$$

Image Noise

All electronic image detectors are subject to stochastic error due to, for example, photon arrival statistics (shot noise), thermally generated electrons, readout electronics, and signal amplification. The shot-noise noise contribution can be reduced by increasing the number of photons detected. This could be accomplished by increasing the scene exposure and/or exposure time. For a CCD-type detector though, the maximum detected signal is limited by its maximum signal (full well) charge. In addition, signal independent dark noise increases as the exposure integration time is increased.[7] Thus any practical system has noise limitations imposed by detector and supporting electronics.

The detected signals, **s**, will include variation from many sources, and can be modeled as a set of random variables. The spectral reflectance and tristimulus vectors will include a corresponding error that will be a function of the variation in **s**, and the matrices **W**, ϕ, and **M** from Eq. (2). Error propagation analysis[8] provides a way of predicting the propagation of the first- and second-order statistics from image detection to transformed signal.

The second-order statistics of a set of detected signals subject to a stochastic error can be described by the covariance matrix,

$$\sum_{\mathbf{s}} = \begin{bmatrix} \sigma_{1,1} & \sigma_{1,2} & \cdots & \sigma_{1,n} \\ \sigma_{2,1} & \sigma_{2,2} & & \\ \cdot & \cdot & & \\ \sigma_{n,1} & \cdot & \cdots & \sigma_{n,m} \end{bmatrix}$$

where the diagonal elements are the variance values of the signals $s_1, s_2, \ldots, s_n$ In general, the elements of $\Sigma_{\mathbf{s}}$ will be functions of the mean detected signal. The resulting covariance matrix for the computed tristimulus vectors is found by[8]

$$\sum_{\mathbf{t}} = \mathbf{W}\phi\mathbf{M} \sum_{\mathbf{s}} [\mathbf{W}\phi\mathbf{M}]^{\mathrm{T}}. \qquad (3)$$

Similarly, the propagation of the signal covariance through nonlinear transformations can be approximated by applying a derivative matrix. If the CIELAB coordinates are expressed as a vector, $\mathbf{c}^{\mathrm{T}} = [L^*, a^*, b^*]$, and the Jacobian Matrix of the multivariate transformation is written as

$$\mathbf{J}_{\mathbf{c}} = \begin{bmatrix} 0 & \partial L^* / \partial Y & 0 \\ \partial L^* / \partial X & \partial a^* / \partial Y & 0 \\ 0 & \partial a^* / \partial Y & \partial b^* / \partial Z \end{bmatrix}$$

then

$$\sum_{\mathbf{c}} = \mathbf{J} \sum_{\mathbf{t}} \mathbf{J}^{\mathrm{T}}. \qquad (4)$$

Note that the derivative terms of Eq. (4) are evaluated at the corresponding mean signal value for each color sample. The error propagation at this step, therefore, will be a dependent on the (mean) signal coordinates.

Experimental Results

From captured images of a MacBeth ColorChecker[9] chart in each of seven image records, the rms pixel-to-pixel noise was computed. The photometric response of the camera was estimated and used to express the camera noise in terms of effective optical exposure variation. This behavior was well modeled by the combination of dark current and shot noise components. Data from all seven filter-records was seen to follow a common characteristic, as shown in Fig. 2.

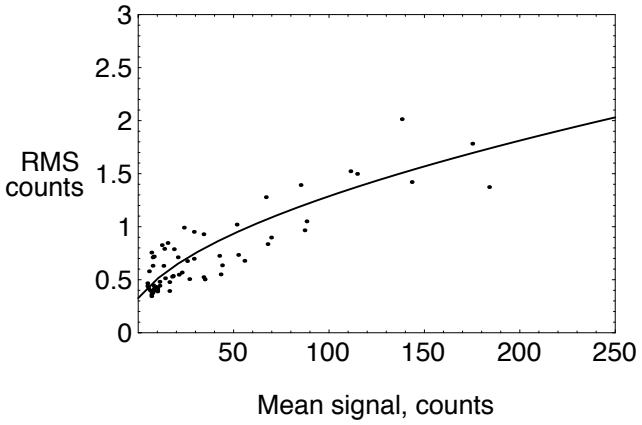

Figure 2: Camera rms noise levels at the detector, expressed as 8-bit digital code values.

The eigenvectors, ϕ, and the least-square matrix, **M** were computed from an independent set of 37 Munsell color samples**.** The spectral reflectance factor of each ColorChecker sample was then estimated from the camera signals, as in Eq. (1). The error propagation analysis of Eqs. (3) and (4) was then applied to the first- and second-order signal statistics for the transformation to CIELAB coordinates.

Despite the fact that the error propagation analysis assumes continuous stochastic error, transformations and their derivatives, the observed signal statistics were well predicted by the analysis. As an example, for the Cyan patch of the MacBeth ColorChecker the CIELAB sample covariance computed from 400 pixel values was

$$\sum_{L^*a^*b^*} = \begin{bmatrix} 0.17 & -0.47 & 0.26 \\ -0.47 & 4.58 & -1.75 \\ 0.26 & -1.75 & 1.71 \end{bmatrix}. \qquad (5)$$

The equivalent statistics propagated via Eqs. (3) and (4) are

$$\sum_{L^*a^*b^*} = \begin{bmatrix} 0.17 & -0.47 & 0.26 \\ -0.47 & 4.59 & -1.76 \\ 0.26 & -1.76 & 1.71 \end{bmatrix} . \qquad (6)$$

The above covariance matrices can be applied to color tolorancing by computing a corresponding confidence ellipsoid. Here, we make a multivariate normal assumption for the error probability density function. Figure (3a) shows the 400 pixel CIELAB data from the above example and Fig. (3b) the 95% confidence ellipsoid based on the covariance matrix of Eq. (6).

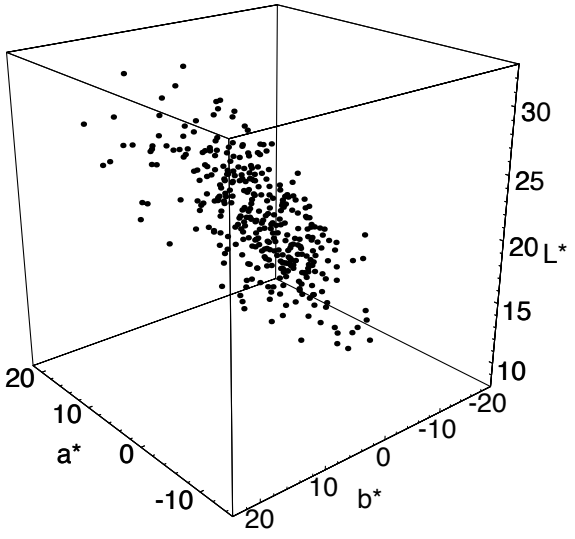

(a)

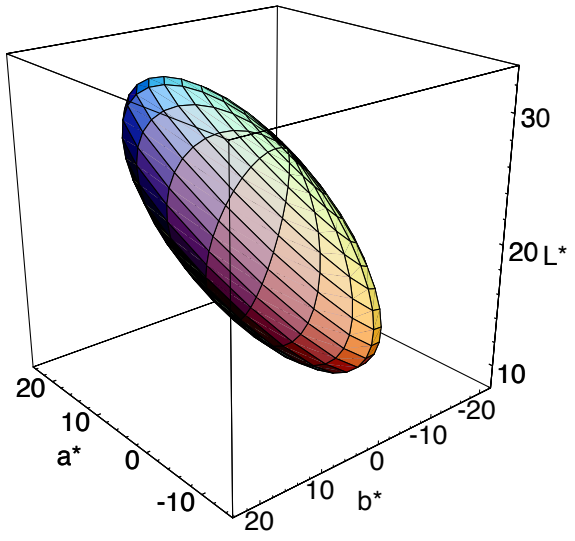

(b)

Figure 3: (a) Distribution of CIELAB coordinates about the mean for the Cyan color sample, based on the camera data from 400 pixels. (b) Corresponding computed 95% confidence ellipsoid based on the CIELAB covariance matrix that was computed via error propagation in Eqs. (3) and (4).

Conclusions

Multispectral image acquisition and the corresponding signal processing have been modeled in a matrix-vector notation. The propagation of stochastic error, from detected signals to colorimetric vectors can then be applied as shown. By including the covariance between the error in each signal, statistical confidence can be established in, for example, CIELAB.

Sources of error such as detector shot noise can depend on signal level, as shown in Fig. (2). Since many transformations applied to color signals are non-linear, the propagation of error will also be signal (level) dependent, as shown in Eq. (4). Combining source modeling and error propagation in this way allows us to predict image noise characteristics, and compare them with those due to, for example, signal quantization.

References

1. M. L. Simpson and J. F. Jansen, 'Imaging Colorimetry: A New Approach,' *Appl. Opt.*, 30: 4666-4671 (1991).
2. K. Martinez, J. Cupitt and D. Saunders, 'High Resolution Colorimetric Imaging of Paintings,' *Proc. SPIE*, 1901: 25-36 (1993).
3. P. L. Vora, M. L. Harville, J. E. Farrell, J. D. Tietz and D. H. Brainard, 'Image Capture: Synthesis of Sensor Responses from Multispectral Images,' *Proc. IS&T/ SPIE Conf. on Electronic Imaging*, 3018: 2-11 (1997).
4. T. Keusen and W. Praefcke, 'Multispecral Color System with an Encoding Format Compatible to Conventional Tristimulus Model,' *Proc. IS&T/SID Third Color Imaging Conf.*, 112-114 (1995).
5. P. D. Burns and R. S. Berns, 'Analysis of Multispectral Image Capture,' *Proc. Fourth Color Imaging Conf., IS&T/SID*, 19-22 (1996).
6. Standard Test Method for Computing the Colors of Objects by Using the CIE System, E 308, American Society for Testing and Materials, NY, latest version.
7. G. C. Holst, CCD Arrays Cameras and Disdplays, JCD Publishing, Winter Park, Florida, 1996, pp. 73-75, 105-112.
8. P. D. Burns and R. S. Berns, 'Error Propagation Analysis for Color Measurement and Imaging,' *Color Research and Appl.*, 22: 280-289 (1997).
9. C. S. McCamy, H. Marcus and J. G. Davidson, 'A Color-Rendition Chart,' *J. Appl. Photogr. Eng.*, 2, 95-99, (1976).